Received: 8 September 2025 | Revised: 1 December 2025 | Accepted: 3 December 2025

DOI: 10.1002/ar.70117

RESEARCH ARTICLE

The Anatomical Record | American Association for Anatomy | WILEY

# An osteohistological analysis of *Triceratops* (Ornithischia: Ceratopsidae) cranial ornamentation

**Kyle D. Obuszewski**[1,2] | **N. Adam Smith**[3] | **Guinevere Rose Brown**[4]

[1]Department of Biological Sciences, North Carolina State University, Raleigh, North Carolina, USA

[2]Paleontology, North Carolina Museum of Natural Sciences, Raleigh, North Carolina, USA

[3]Negaunee Integrative Research Center, Field Museum of Natural History, Chicago, Illinois, USA

[4]South Carolina Department of Environmental Sciences, Columbia, South Carolina, USA

**Correspondence**
Kyle D. Obuszewski, Department of Biological Sciences, North Carolina State University, Campus Box 7617, Raleigh, NC 27695, USA.
Email: kdobusze@ncsu.edu

## Abstract

Ceratopsids are among the most distinctive and well known extinct Cretaceous vertebrates, yet many details regarding the growth and composition of their cranial features are still not fully anatomically described or understood. In particular, striking cranial adornments such as the postorbital horns and parietal-squamosal frill of *Triceratops* experience a series of major morphological and histological shifts throughout ontogeny. While previous osteohistological studies have largely focused on the parietal of *Triceratops*, there are relatively few studies of postorbital horn and squamosal histology. Here we present an in-depth osteohistological description of the postorbital horns and squamosal from a single subadult *Triceratops horridus* specimen and compare similar histological features among ceratopsian cranial ornaments. Analysis revealed the postorbital horns display considerable histological variation based on sampling location, with our proximal section describing an extensive range of vascularity across three notable horizons previously undocumented, suggesting that histological ontogenetic assessments could differ across ornamental structures. Although the *Triceratops* squamosal maintains similarities with remodeled bone among other ceratopsid parietals, distinct growth marks are preserved near the periosteal surface containing at least three lines of arrested growth, citing a novel developmental shift from rapid azonal to slowed zonal growth late in ontogeny. Additionally, although some metrics of cranial size remain relatively unreliable characteristics for assessing ontogeny, occipital condyle dimensions may offer an avenue of delineating ontogenetically older *Triceratops* individuals. Alongside morphological measurements, extensive histological sampling may provide a means to clarify currently perceived anatomical inconsistencies and heterochronic variation between putative adults and subadults of *Triceratops* and other ceratopsids.

**KEYWORDS**

ceratopsid, histology, ontogeny, ornamentation

## 1 | INTRODUCTION

*Triceratops* represents one of the largest and most common ceratopsids during the latest Cretaceous of western North America. Of the 16 originally described species, only 2 species of *Triceratops* are currently recognized: *T. horridus* and *T. prorsus* (Forster, 1996a; Marsh, 1889), both commonly described by their unique cranial morphology (Farke et al., 2009; Forster, 1996b; Goodwin et al., 2006; Hatcher et al., 1907; Horner & Goodwin, 2006, 2008; Marsh, 1889; Scannella & Horner, 2010). In particular, the postorbital horns and parietal-squamosal frill of *Triceratops* are excellent indicators of morphological change throughout ontogeny (Goodwin et al., 2006; Horner & Goodwin, 2006; Scannella & Horner, 2010). In juveniles, the frill is short and boxy, deeply scalloped along the frill border, and slightly bent in the squamosal region, while the postorbital horns are short and nondirectional (Goodwin et al., 2006; Horner & Goodwin, 2006). Larger juveniles nearly double the length and width of the frill, and the horns grow into a posterior-facing orientation (Horner & Goodwin, 2006; Horner & Lamm, 2011). Growth begins to slow in *Triceratops* subadults as the postorbital horns transition to an anterior-facing orientation and the frill surface develops a rugose texture (Horner & Goodwin, 2006; Longrich & Field, 2012). Mature adults are characterized by a short and broad parietal-squamosal frill containing dorsoventrally flattened epiparietals and episquamosals fused along the frill margin and lacking parietal fenestrae (Hatcher et al., 1907; Horner & Goodwin, 2006).

Given the developmental complexities of ceratopsid ornamentation, morphological indicators represent only one axis of identifying ontogeny in *Triceratops*. Although cranial sutures are also key indicators for skeletal maturity (Fujiwara & Takakuwa, 2011; Longrich & Field, 2012), they require articulated cranial material to be informative. Alternatively, osteohistology has become an increasingly popular method of assessing ontogeny in non-avian dinosaurs. Although some early diverging members have been sampled (Baag & Lee, 2022; Chinnery & Horner, 2007; Han et al., 2024; Napoli et al., 2019; Skutschas et al., 2021; Zhao et al., 2019), most ceratopsian histological studies have focused on more derived members of the clade, namely ceratopsids (D'Anastasio et al., 2022; de Rooij et al., 2024; Hedrick et al., 2020; Horner & Lamm, 2011; Ishikawa et al., 2023; Lehman et al., 2017; Scannella & Horner, 2010; Tumarkin-Deratzian, 2010). Some cranial elements of *Triceratops* have been histologically sampled, with most studies gravitating towards cranial ornamentation, particularly the parietal frill (Horner & Lamm, 2011; Scannella & Horner, 2010). Ontogenetic characters of the *Triceratops* frill have been documented to describe changes in frill thickness, generate ontogenetic growth series, argue for the ontogenetic trajectory hypothesis (OTH), and assess frill pathologies alongside potential evidence of intraspecific combat (D'Anastasio et al., 2022; Farke, 2011; Horner & Lamm, 2011; Scannella & Horner, 2010, 2011). More recently, histologic ontogenetic stages (HOS) were proposed for *Triceratops* through an array of postcranial histological samples (de Rooij et al., 2024). However, the application of non-parietal ornamental histology, specifically from the postorbital horns and squamosal, is comparatively limited (D'Anastasio et al., 2022; Scannella & Horner, 2010). Since Scannella and Horner (2011), no further published osteohistological analyses have been conducted on *Triceratops* postorbital horn material.

Size has also been used to assess relative ontogenetic age in *Triceratops*, despite considerable intra-specific variation in the relationship between size and ontogenetic age within Dinosauria (Atterholt & Woodward, 2021; Chinsamy-Turan, 2005; Frederickson & Tumarkin-Deratzian, 2014; Longrich & Field, 2012; Mallon et al., 2022; Sander & Klein, 2005; Starck & Chinsamy, 2002). Although the size of cranial elements is generally correlated with ontogenetic age in ceratopsids (Frederickson & Tumarkin-Deratzian, 2014; Scannella et al., 2014; Scannella & Horner, 2010), differentiating between individuals of similar sizes, particularly between subadults and adults, can be challenging (Frederickson & Tumarkin-Deratzian, 2014; Longrich & Field, 2012). HOS have also been shown to correlate with body size (Klein & Sander, 2008), including in *Triceratops* (de Rooij et al., 2024). The inclusion of more histological ontogenetic stages for *Triceratops* (seven) in de Rooij et al. (2024) than the morphological stages (four) proposed by Horner and Goodwin (2006) could allow size to become a more reliable estimate of ontogeny. As it currently stands, however, the correlation between size and ontogenetic stage among more skeletally mature individuals remains unclear.

We examined the osteohistology of a pair of postorbital horns and a right squamosal from a subadult *T. horridus* specimen, BCGM 10272, to refine the relationship between cranial osteohistology, size, and ontogeny in *Triceratops*. We identified the postorbital horn osteohistological profile for BCGM 10272 by utilizing the short growth series provided by Scannella and Horner (2010) and contrasted microanatomical features between the squamosal and parietal aspects of the *Triceratops* frill. To assess the uncertainty of size as a late ontogenetic character for some ceratopsians, we generated several statistical plots to correlate ontogeny and cranial measurements across previously measured *Triceratops* specimens.

*Institution abbreviations*: AMNH, American Museum of Natural History, New York City, NY, USA; BCGM, Bob Campbell Geology Museum, Clemson, SC, USA;

BSP, Bayerischen Staatsammlung für Geologie und Palieontologie, Munich, Germany; CM, Carnegie Museum of Natural History, Pittsburg, PA, USA; FMNH, Field Museum of Natural History, Chicago, IL, USA; LACM, Natural History Museum of Los Angeles County, Los Angeles, CA, USA; MOR, Museum of the Rockies, Bozeman, MT, USA; SMM, Science Museum of Minnesota, St. Paul, MN, USA; UCMP, University of California Museum of Paleontology, Berkeley, CA, USA; USNM, United States National Museum of Natural History, Washington, DC, USA; UTEP, University of Texas at El Paso (Centennial Museum), El Paso, TX, USA; YPB, Yale Peabody Museum, New Haven, CT, USA.

## 2 | MATERIALS AND METHODS

BCGM 10272 was recovered from the Hell Creek Formation in western North Dakota in 2017 and is represented by an associated partial skull, most notably including partial left and right horncores, a right squamosal, and a partial braincase (Figures 1 and 2 , Data S1). All elements were found in partial articulation and prepared from two field jackets that were taken from an area less than two square meters. One jacket contained the partial braincase, and the other contained the right squamosal, both horncores, a partial rib, and a tooth. There is no evidence suggesting the elements are representative of multiple individuals. Previous analyses utilized the dimensions of the occipital condyle across *Triceratops* to assign BCGM 10272 as a subadult individual (Brown & Smith, 2017). Due to the incomplete and fragile nature of both horns, complete circumferential cross-sections were unobtainable, and instead partial transverse cross sections were sampled from the tentatively assigned medial border of both postorbital horns (Figure 1). Additionally, because of their aforementioned preservation, the left and right horncores were sampled at different proximo-distal lengths, with the left horn section stemming from a more distal position (i.e., closer to the horn tip) relative to the right horn section (Figure 1). A similar approach was employed for the right squamosal, as a small, isolated fragment was sampled for a transverse section (Figure 2), with most of the preparation work performed by the National Petrographic Service. The left and right postorbital horn sections were removed using a circular diamond blade saw and embedded in an epoxy resin. The resin blocks were then trimmed and mounted to frosted glass slides, ground on a lap wheel with various grit papers to a preferable contrast between 20 and 200 microns thick, and polished. All thin sections were examined with a Nikon Eclipse Ci-Pol polarizing microscope under plane-polarized light, cross-polarized light, and cross-polarized light with a 530-nm lambda filter. Each section was photographed using a Nikon DS-Ri2 camera at 20×, 40×, and 100× total magnification where necessary. Composite images were photographed and stitched with a Keyence VHX-7000 digital microscope at

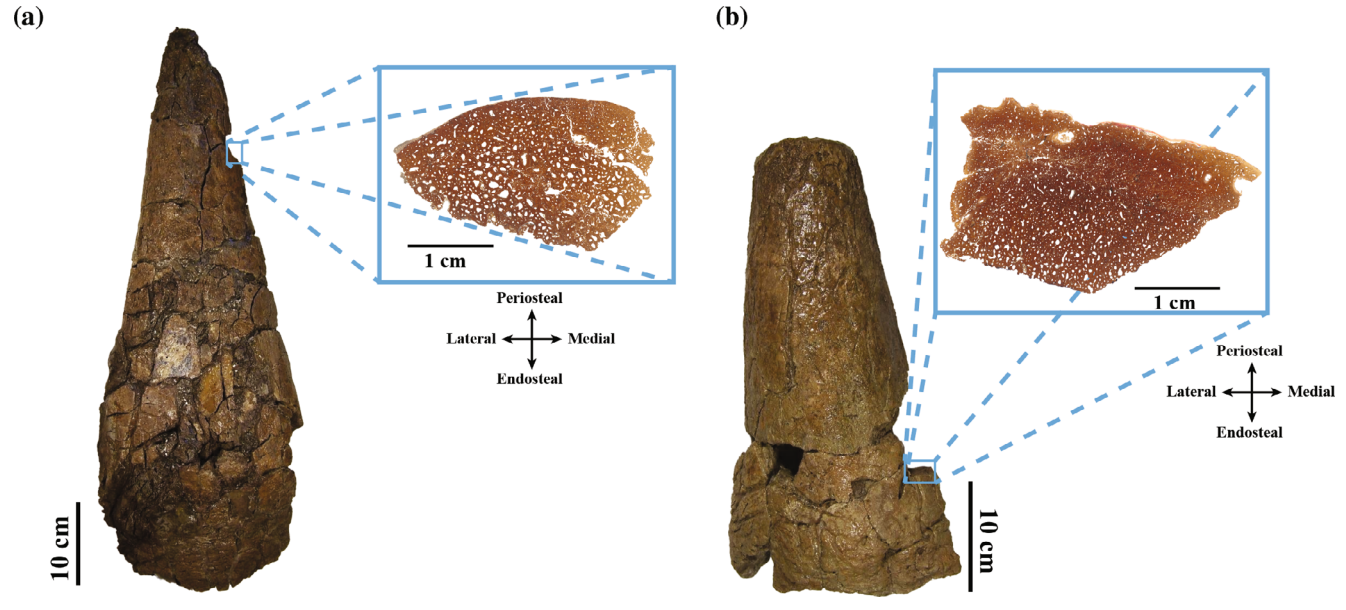


FIGURE 1 Postorbital horns of BCGM 10272. (a) Left postorbital horn in dorsal view. (b) Right postorbital horn in ventral view. The smaller rectangles indicate the location of histological sampling, and the larger rectangles contain stitched images of each section under plane-polarized light at 7.6× total magnification. Orientations are shown for each section. Scale bars for each horn and histological sample are 10 cm and 1 cm, respectively.

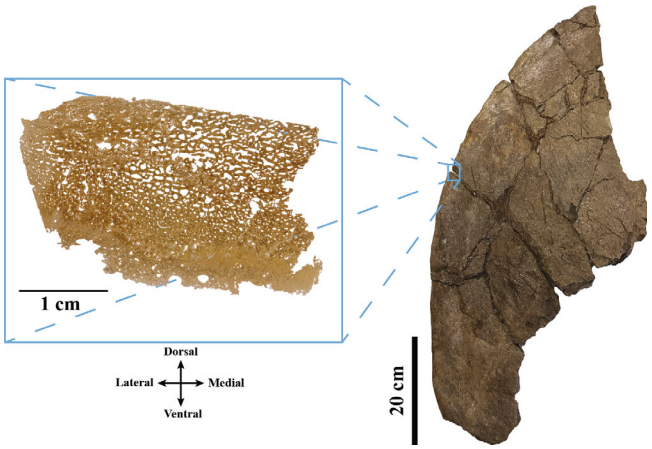


**FIGURE 2** Right squamosal of BCGM 10272 in dorsal view. The smaller rectangle indicates the location of histological sampling, and the larger rectangle contains stitched images of the squamosal section under plane-polarized light at 7.6× total magnification. Orientations are shown below the section. Scale bars for the squamosal and histological sample are 20 cm and 1 cm, respectively.

7.6× total magnification. Where appropriate, bone tissue thicknesses were conservatively estimated and mapped, in which mapped primary bone tissues do not include any remodeled sections.

Cranial measurements and ontogenetic age assignments were sampled from BCGM 10272 and 41 *Triceratops* specimens established within the literature (Data S2) (Anderson, 1999; Brown & Smith, 2017; Forster, 1996b; Horner & Goodwin, 2006; Longrich & Field, 2012; Maiorino et al., 2013; Scannella et al., 2014; Scannella & Horner, 2010). We follow the original naming scheme provided by Horner and Goodwin (2006) to categorize morphological ontogenetic stages into four bins: "Baby," "Juvenile," "Subadult," and "Adult." Most *Triceratops* ontogenetic studies sampled follow this method except for Scannella and Horner (2010), which introduced a fifth stage ("Young adult") to include all previously identified "Adult" *Triceratops* specimens and instead assigned all sampled *Torosaurus* specimens as "Adult" *Triceratops* individuals. Since then, several studies have argued that there is substantial evidence for ontogenetic variation in *Torosaurus* morphology and osteohistology to consider the genus distinct from *Triceratops* (Farke, 2011; Longrich & Field, 2012; Maiorino et al., 2013; Mallon et al., 2022), despite a limited histological sample size (de Rooij et al., 2024). As such, *Torosaurus* specimens were not included in this analysis. Specimens labeled as an "Adult" in Scannella and Horner (2010) were excluded, and those labeled as "Young adult" specimens were considered adults for this study. Statistical analyses were plotted at the generic level, incorporating *T. horridus*, *T. prorsus*, and indeterminate *Triceratops* specimens. Although *T. prorsus* has been recognized by having a smaller postorbital horn length relative to skull length compared to *T. horridus*, among other features (Forster, 1996b), the four *T. prorsus* specimens we included do not have postorbital horn measurements listed within the literature, and no other measurements relating to their diagnosable differences were included. BCGM 10272 cranial measurements were taken twice using digital calipers and a measuring tape, where appropriate, and then averaged. Basal skull length refers to the distance between the rostral and posterior surface of the occipital condyle. When not provided in the literature, the area of the occipital condyle was manually calculated as the product of the width and height.

Simple linear regression models and boxplots were plotted in RStudio version 4.4.1 with the R-packages "ggplot2" and "ggsignif" (Ahlmann-Eltze & Patil, 2021). Plots were produced for the following cranial measurements: basal skull length, postorbital horn length, occipital condyle width, occipital condyle height, and occipital condyle area. For linear regression models, each cranial measurement was plotted against basal skull length, after log transforming both metrics (Data S1). Boxplots were generated to test significant differences among the distributions of cranial measurements by morphological ontogenetic stage. Measurements for parietal and squamosal length were also sampled; however, due to smaller sample sizes ($n = 9$, 12 for parietal and squamosal length, respectively) and differences in recorded measurements between left and right squamosals of some specimens, they were excluded from final analyses. Their linear regression models, as well as models in which we exclusively sampled specimens without estimated cranial measurements, are available in Data S1.

## 3 | RESULTS

The postorbital horns of BCGM 10272 are heavily remodeled, composed primarily of azonal secondary bone. Both horns contain a mixture of dense and loosely packed Haversian tissue, with the latter lined by interstitial tissue (Figures 3b–d and 5b), and osteons tend to follow a longitudinal orientation. While the left horn is entirely composed of Haversian tissue (Figure 3a–d), the cortex of the right horn is composed of three distinct tissue horizons that exhibit dynamic vascular maturity (Figures 4a–c and 5a,b). Secondary bone, intermittent with interstitial tissue, forms the lowest and most extensive horizon of the right horn cortex. Superficially, a somewhat thin band of fibrolamellar bone persists with plump osteocyte lacunae, randomly oriented collagen fibers, and primary osteons (Figures 4b,c and 5c). The third and

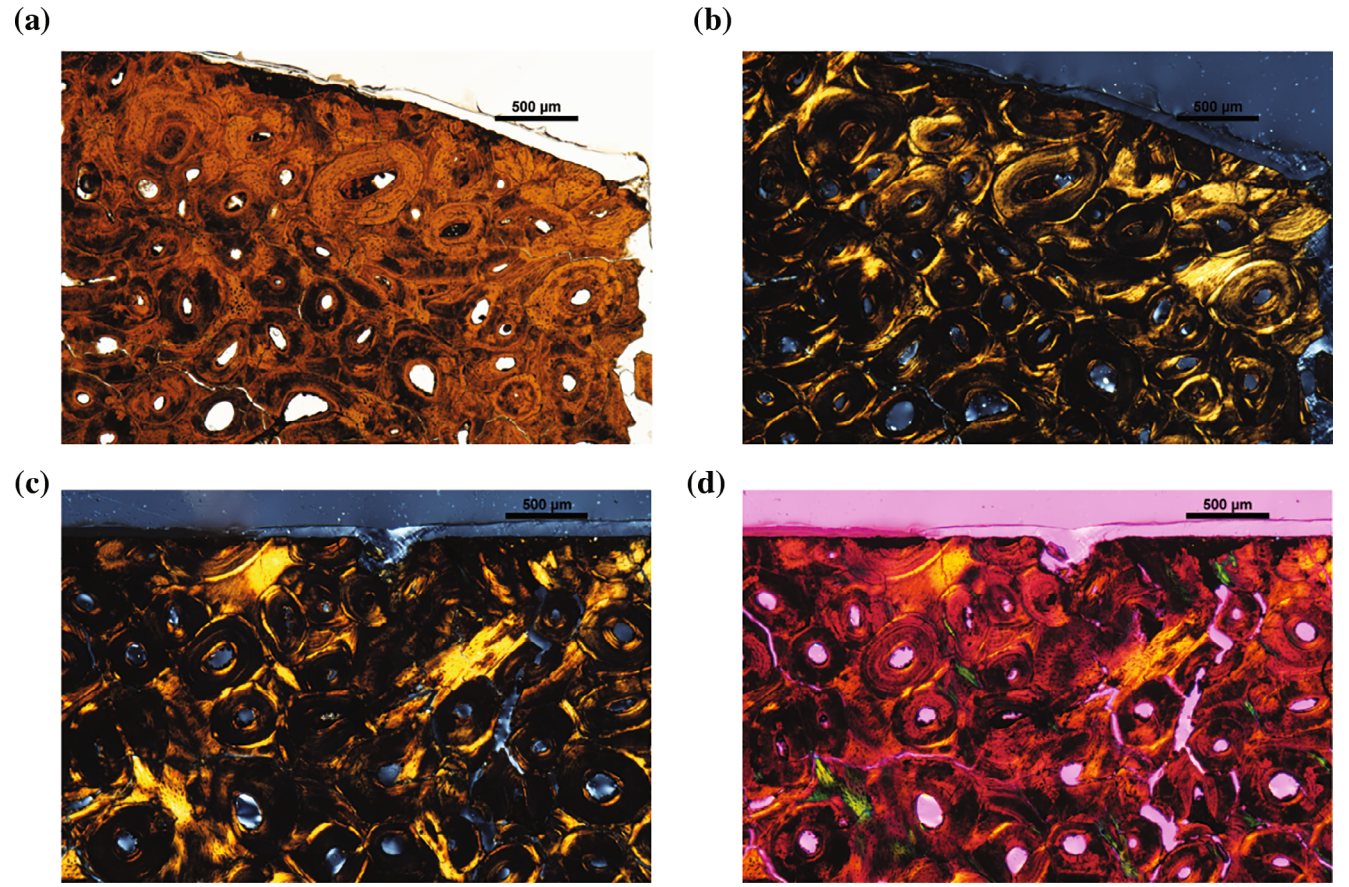


**FIGURE 3** Left postorbital horn histology of BCGM 10272. (a, b) Medial periosteal surface in plane-polarized light (a) and cross-polarized light (b). (c, d) Mid-line periosteal surface in cross-polarized light without (c) and with (d) a lambda filter. All four images contain secondarily remodeled bone at the periosteal surface.

final horizon, composed of low vascularity parallel-fibered bone, contains tightly packed collagen fibers that extend across the entire periosteal surface (Figures 4a and 5a,b). Although the relative extent of secondary bone is consistent, the thickness of the upper two horizons varies across the right horn, especially in portions of fibrolamellar bone that are actively being remodeled (Figure 5b). Regardless of layer thickness, all three horizons are present throughout the entire section of the right horn. Neither horn displays evidence of an external fundamental system (EFS), indicated by lamellar bone or growth marks at the periosteal surface.

The right squamosal of BCGM 10272 is also heavily remodeled, containing both secondary cancellous and compact bone, and osteons predominately follow a longitudinal orientation. However, there is differentiation within the secondarily remodeled cortex between dense and loosely packed Haversian bone with density of secondary osteons decreasing and abundance of parallel-fibered interstitial tissue increasing periosteally (Figure 6a,b). Several segments of primary bone, albeit incomplete, are preserved ventrally containing a mixture of woven-fibered and lamellar matrices surrounding simple vascular canals and primary osteons (Figures 2 and 7a,b). Although distinct uninterrupted annuli do not appear to be present, at least three identifiable lamellar bands are present with varying preserved lengths running roughly parallel along the overlying periosteal surface (Figure 7a,b).

There is a strong correlation ($R^2 \geq 0.95$) between various cranial measurements and basal skull length in *Triceratops* (Data S1). The only exception is the correlation between postorbital horn length and basal skull length, though the correlation is still fairly strong ($R^2 = 0.84$). When compared with ontogenetic stage, cranial size has a more nuanced relationship, displaying a roughly stepwise progression across all measurements (Figure 8a–e). While basal skull length and postorbital horn length are not significantly different between subadults and adults, all three occipital condyle measurements (width, height, and area) appear to be robust indicators of maturity among older individuals ($p = 0.05$, 0.014, and 0.019, respectively) (Figure 8c–e).

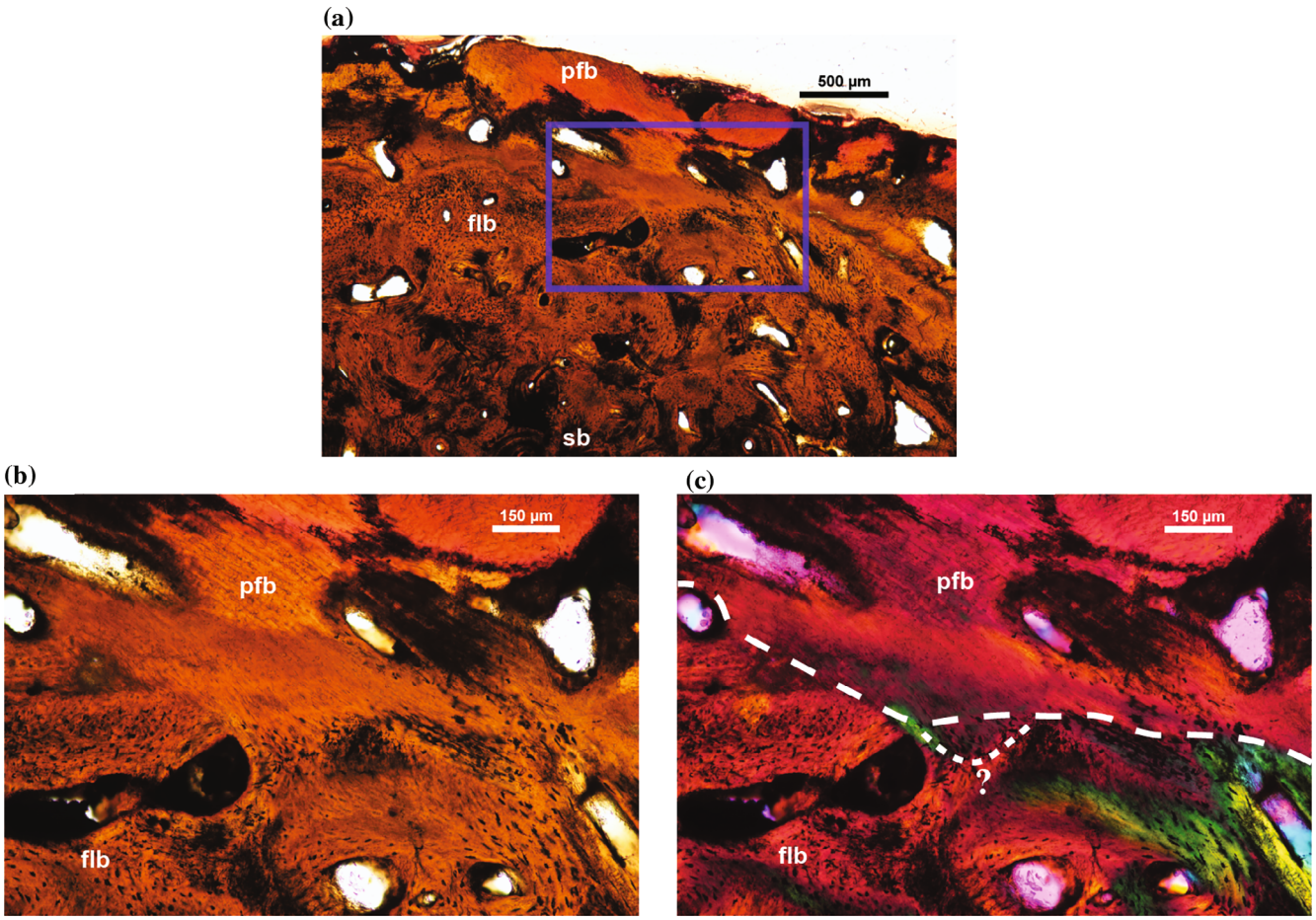


**FIGURE 4** Right postorbital horn histology of BCGM 10272. (a) Fibrolamellar and parallel-fibered bone contact near the mid-line periosteal surface in plane-polarized light. (b, c) Close-up of the fibrolamellar and parallel-fibered bone contact, mapped by the dotted lines, in plane-polarized light (b) and cross-polarized light with a lambda filter (c). Uncertainty in the contact is indicated by shorter dashes above the question mark. flb, fibrolamellar bone; pfb, parallel-fibered bone; sb, secondary bone.

## 4 | DISCUSSION

The postorbital horn osteohistology of BCGM 10272 unveils previously undocumented nuances to *Triceratops* horncore development. Whereas high vascularization has been reported within the postorbital horns of all *Triceratops* morphological ontogenetic stages (Scannella & Horner, 2010), and is supported here, the presence of three distinct horizons of fast- and slow-growing bone tissues in the right horn of BCGM 10272 suggests an appositionally dynamic growth strategy. Of the three horizons, the outermost parallel-fibered bone is surprising to find in BCGM 10272 and demonstrates a drastic shift in periosteal vascularization and growth, in conjunction with secondary remodeling. However, this does not constitute an EFS characterized by subperiosteal lamellar bone (Padian et al., 2013), and has not been reported in *Triceratops* cranial ornamentation or any ceratopsid postorbital horn (Horner & Lamm, 2011; Lehman et al., 2017; Scannella & Horner, 2010). Currently, it is unknown whether ceratopsid postorbital horns follow a determinate or indeterminate growth strategy through ontogenetic maturity, complicating relative ontogenetic age assessments. In addition, the case of histological maturity in BCGM 10272 specifically is exacerbated by differing positions of histological sampling in both horns, each arguing for a different assignment of maturity. Although secondary bone is dominant throughout the right horn, a combination of fibrolamellar and parallel-fibered bone, encompassing primary bone, is consistent with a "Subadult" ontogeny (Scannella & Horner, 2010). However, the homogenous Haversian tissue within the left horn is more supportive of an "Adult" ontogeny (Scannella & Horner, 2010). The left horn of BCGM 10272 is slightly longer and more distal in preservation than the right horn and, given the fragile and incomplete nature of both horns, we were unable to sample roughly equivalently along their proximal-distal length. In addition, the ossification center of *Triceratops* postorbital horns has long been hypothesized to originate at the base of each

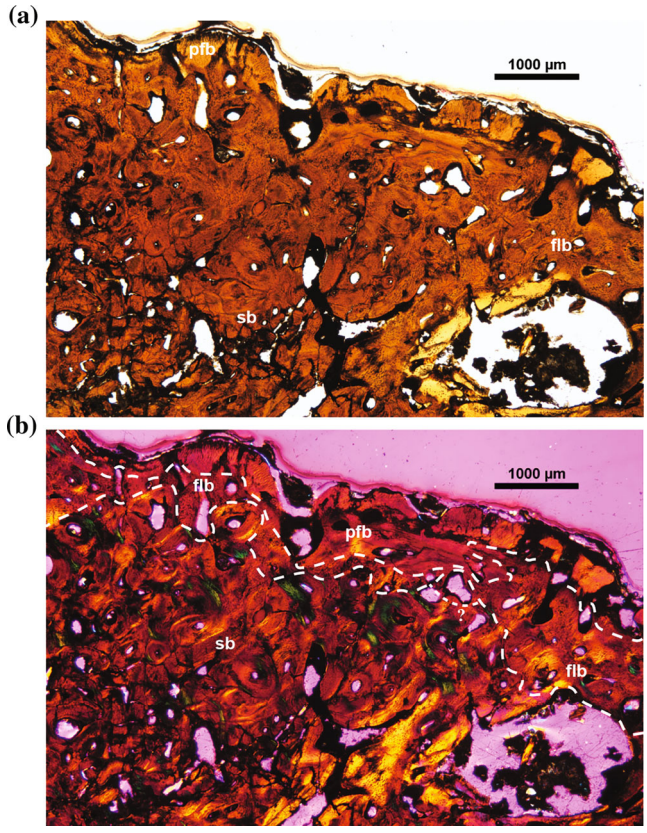


FIGURE 5 Histological profile for the right postorbital horn of BCGM 10272. (a, b) Periosteal surface near the lateral edge of the section in plane polarized light (a) and cross-polarized light with a lambda filter (b). Tissue types are mapped with dashed lines. Uncertainty between contacts is indicated by shorter dashes above the question mark. flb, fibrolamellar bone; pfb, parallel-fibered bone; sb, secondary bone.

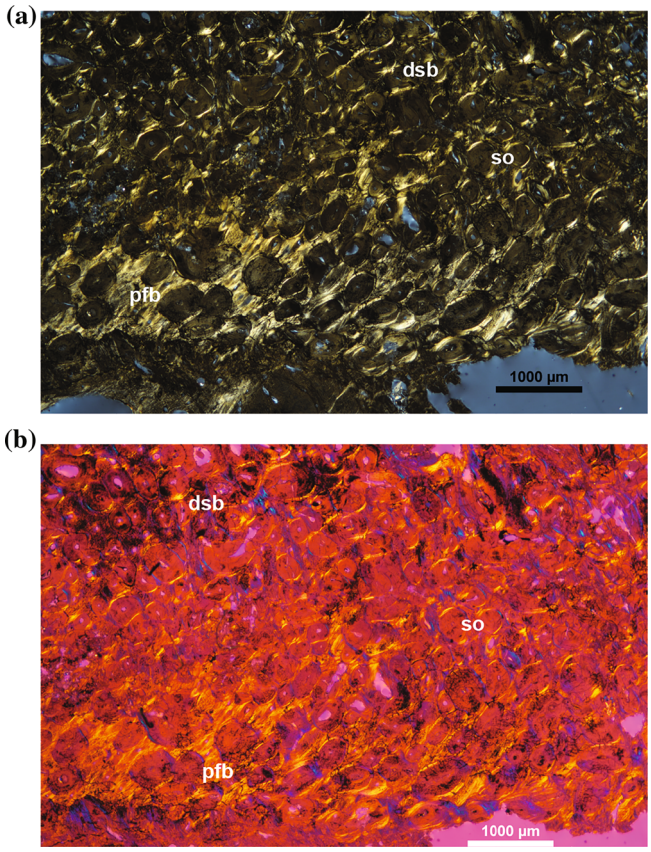


FIGURE 6 Right squamosal histology of BCGM 10272. (a, b) Haversian bone interwoven with interstitial parallel-fibered bone near the ventromedial surface of the section in cross-polarized light without (a) and with a lambda filter (b). dsb, dense secondary bone; pfb, parallel-fibered bone; so, secondary osteons.

horncore (Hatcher et al., 1907), although no histological analyses have tested for a stratified histological age profile. Previous horncore histology from two *Agujaceratops* specimens proposed that one juvenile specimen (UTEP P.37.7.379) preserves recognizable growth marks across two sections, and argued that greater remodeling in a proximal section from a larger horn (UTEP P.37.7.380) supports slower growth near the horncore base (Lehman et al., 2017). Nevertheless, both juvenile sections represent macroscopic cross-sections, and without finer resolution, it is unclear whether lines of arrested growth (LAGs) are truly present or if the proposed modulations are simply taphonomic. Additionally, our results and Scannella and Horner (2010) show no evidence for any growth marks or LAGs within any *Triceratops* horncores regardless of growth stage, including juveniles. Contrary to Lehman et al. (2017), our results also indicate that postorbital horn growth may have slowed distally instead of proximally, with the distal end of the left horn containing an entirely remodeled interior. Alternatively, differences in the left and right horncore histology of BCGM 10272 may be attributable to taphonomic degradation of the periosteal surface. If present, then the left horncore section could provide an overestimation of age by preserving only heavily remodeled secondary bone. However, gross inspection of the left horn sampling location does not reveal any evidence of weathering or deformation, and, although we cannot say degradation was truly impossible, we see no evidence suggesting that our histological interpretations are impacted by taphonomy. A more thorough study of *Triceratops*, and ceratopsid, horncore histology is needed to address both the absence of an EFS and the potential for histological variation along horncore length within a single individual.

The squamosal is a seldom published element for ceratopsian histological analyses (D'Anastasio et al., 2022; Tumarkin-Deratzian, 2010); however, we can contextualize the squamosal of BCGM 10272 relative to a series of sampled *Triceratops*, *Torosaurus* (Horner & Lamm, 2011), and *Centrosaurus* (Tumarkin-Deratzian, 2010) parietals. The highly remodeled squamosal cortex of BCGM 10272 is

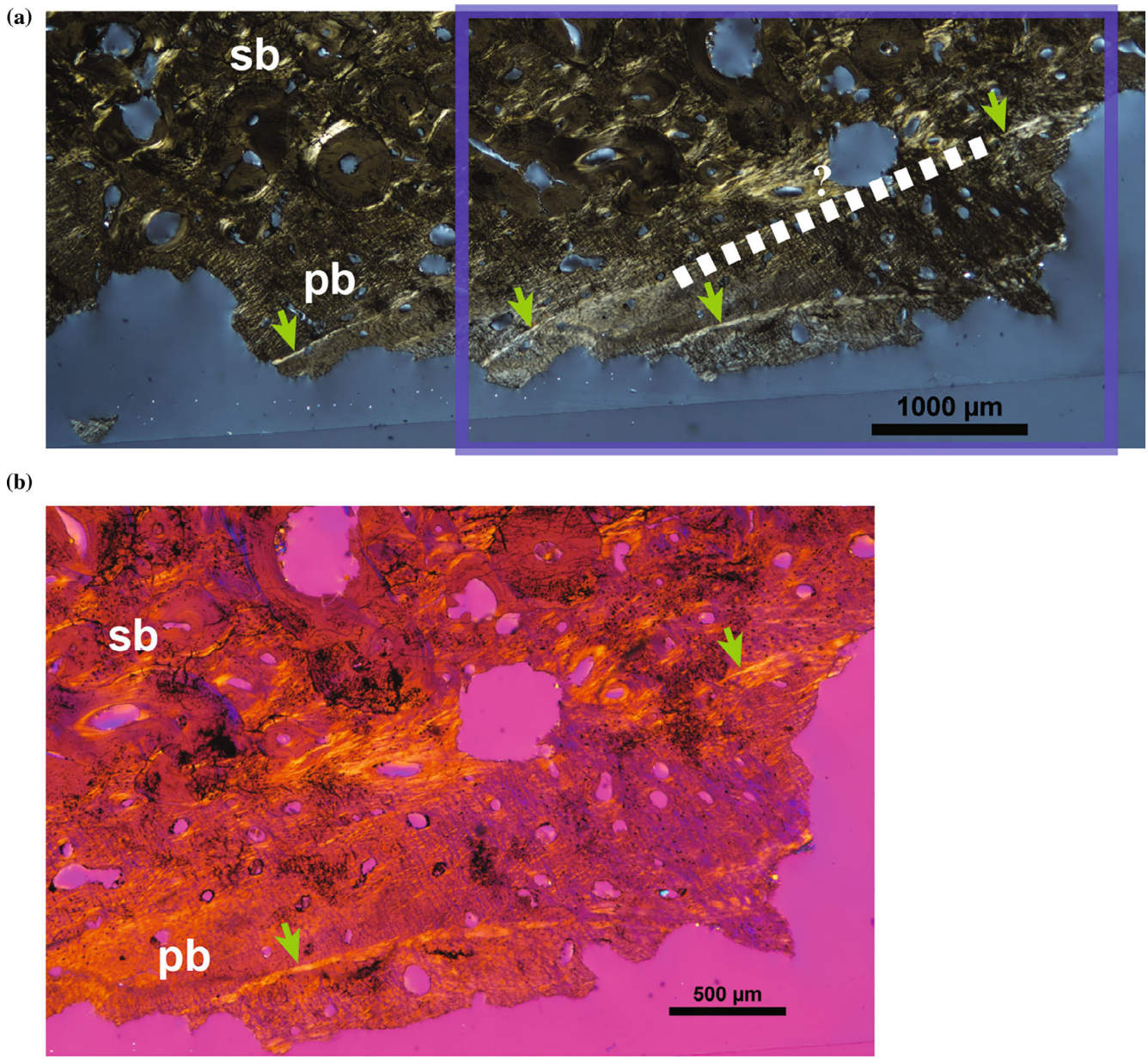


**FIGURE 7** Lamellar tissue in the right squamosal of BCGM 10272. (a) Combination of primary and secondary bone, with the former containing at least three distinct bands of lamellar tissue, along the ventral (periosteal) mid-line in plane-polarized light. Green arrows highlight each lamellar section. The dashed lines indicate the hypothesized extent of the second lamellar band. (b) Close-up of the two ventral-most lamellar bands in cross-polarized light with a lambda filter. pb, primary bone; sb, secondary bone.

generally characteristic among more ontogenetically mature individuals, but the presence of primary bone tissue indicates that the frill was actively growing prior to fossilization. Besides BCGM 10272, secondary osteons interwoven with parallel-fibered tissue have also been described near the ventral surface of *Torosaurus* parietal MOR 981 (Horner & Lamm, 2011), implying some similarity among ceratopsid frill growth strategies. Although densely fibered matrices are known from the parietal of several more skeletally mature *Triceratops* and *Torosaurus* individuals (Horner & Lamm, 2011), BCGM 10272 represents only the second instance of definitive lamellar bone found within ceratopsid frills, after *Centrosaurus* (Tumarkin-Deratzian, 2010). Metaplastic connective tissue has been argued to develop late in parietal frill ontogeny to help accommodate the eventual fusion of epiparietals to the frill margin as evidenced by mineralization zones within MOR 981 (Horner & Lamm, 2011); however, the full longitudinal extent of these zones is unclear and the lamellar bands in BCGM 10272 appear more extensive in length (at least 2–3× the length in MOR 981) and width, to some extent. The lamellar bands in BCGM 10272 can also be differentiated

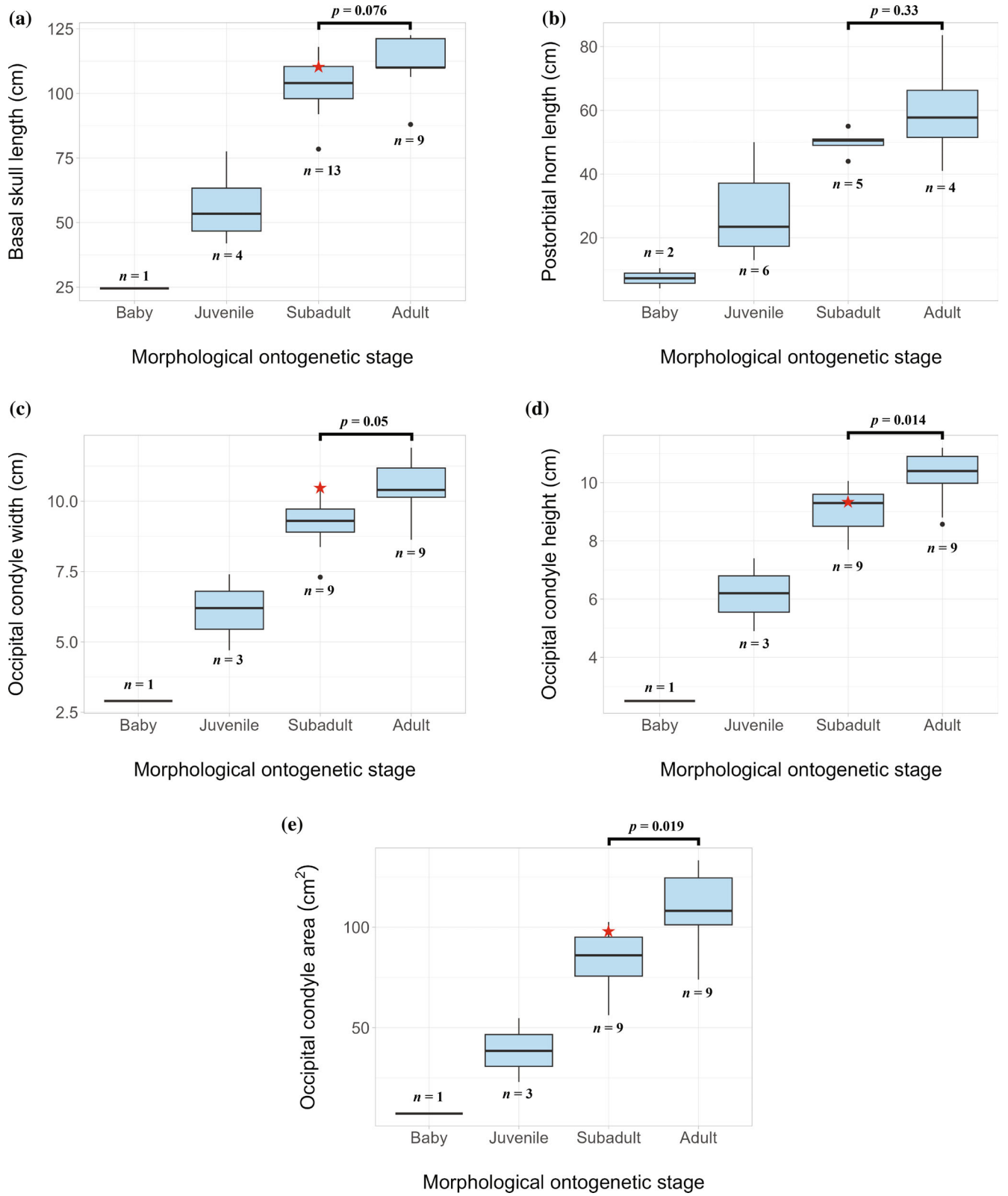


**FIGURE 8** Comparisons of *Triceratops* assigned morphological ontogenetic stages with basal skull length (a), postorbital horn length (b), occipital condyle width (c), height (d), and area (e). Red stars highlight the position of BCGM 10272, and *p*-values indicate significance tests of observed cranial distinctions between subadults and adults. Sample sizes for each ontogenetic bin are shown with each boxplot.

from lamellar tissues in *Centrosaurus* that instead form a signature EFS (Tumarkin-Deratzian, 2010). As such, we tentatively assign the three linear bands of lamellar tissue in BCGM 10272 as LAGs, suggesting a transition from rapid azonal to slower zonal growth within the squamosal near skeletal maturity. However, due to taphonomic processes we are missing some of the ventral-most extent of the squamosal, limiting our interpretation of potential growth mark expansion laterally and periosteally. Additionally, bone flaking along thinner portions of the ventral surface (Anné and Tumarkin-Deratzian, personal communication) precludes our ability to identify potential annuli, or lack thereof, between LAGs.

Traditionally, cranial measurements have been used to estimate basal skull length in *Triceratops* (Anderson, 1999; Forster, 1996b; Horner & Goodwin, 2006; Scannella et al., 2014). Although cranial measurements represent a simple and non-invasive method for assessing relative ages among ceratopsids and are strongly correlated with basal skull length in *Triceratops* (Scannella et al., 2014), size is less reliable for assessing ontogeny. Mature ceratopsids greatly vary in body size (Longrich & Field, 2012) and although comparisons among ontogenetically younger individuals are fairly clear-cut, some cranial discrepancies appear between *Triceratops* subadults and adults (Figure 8a,b). Despite displaying a roughly stepwise progression, subadult and adult specimens are variable across several cranial measurements and display statistically similar interquartile ranges for some measurements (Figure 8a,b). However, the distribution of occipital condyle measurements across more skeletally mature individuals is significantly different (Figure 8c–e), suggesting that the braincase may be a more reliable indicator of ontogeny than previously thought.

Morphological characteristics, particularly cranial ossifications, provide more accurate ontogenetic evaluations compared to size (Fujiwara & Takakuwa, 2011; Longrich & Field, 2012). However, there are still inconsistencies between differentiating subadults and adults, especially among *Triceratops* and *Torosaurus* skulls that contain a series of mature and immature features (Longrich & Field, 2012; Mallon et al., 2022). As an additional supplement, histology can provide a means for accurately assessing relative ontogenetic age within *Triceratops*, particularly when specimens are fragmentary or lacking in key morphological indicators of ontogeny. With recent histological work done by de Rooij et al. (2024), a framework for connecting *Triceratops* morphological and histological ontogenetic stages has become more established, at least for postcranial sampling. However, we refrain from assigning the horns or squamosal of BCGM 10272 to a HOS due to differences in histological sampling, regarding the location of sampled elements and overall methodology. As such, we tentatively retain a subadult ontogenetic age for BCGM 10272. Moreover, we recommend caution when labelling ontogenetic ages based on ornamental histology, especially for ceratopsids. There is a significant gap between intraspecific and interspecific ornament histological sampling across late branching ceratopsians that needs to be addressed before any cranial histological stages can be established or substantially compared with our existing record. For postorbital horn histology specifically, questions of intraspecific and proximo-distal variation remain unanswered due to an incredibly poor database of, to our knowledge, only two sampled ceratopsid taxa (*Agujaceratops* and *Triceratops*). Parietal-squamosal frill histology suffers from similar uncertainties with generalizations of frill histological growth for chasmosaurines and centrosaurines stemming primarily from *Triceratops* and *Centrosaurus*, respectively (Horner & Lamm, 2011; Tumarkin-Deratzian, 2010). More extensive sampling of *Triceratops* and ceratopsid ornamentation is necessary to elucidate the development of display characters across Ceratopsidae and test their utility in identifying measures of maturity.

## 5 | CONCLUSIONS

*Triceratops* maintains itself as an incredibly critical taxon for resolving morphological, phylogenetic, and ontogenetic ambiguities among late branching ceratopsians and our results provide a much-needed reassessment of their ornamental histology. The postorbital horn osteohistology of BCGM 10272 exhibits greater intraspecific variability than previously expected in *Triceratops*, with the proximal right horn section containing a dynamic range of vascularity compared with the entirely remodeled distal left horn section, suggesting that assessments of ontogenetic maturity may differ across cranial ornaments. *Triceratops* squamosal microanatomy shares some similarities with previously sampled parietal sections but deviates greatly in the presence of distinct lamellar bands interpreted as lines of arrested growth, documenting a dramatic shift in frill development approaching skeletal maturity. Occipital condyle measurements appear to be robust delineators of skeletal maturity in *Triceratops*, restoring usefulness in some morphological indicators of ontogeny beyond cranial sutures. A combination of morphological and histological tools is essential to address seemingly cryptic diversity among ontogenetically mature individuals across Ceratopsidae. However, a greater framework of ceratopsid histology must be established before sweeping conclusions can be made about display character heterochrony.

## AUTHOR CONTRIBUTIONS

**Kyle D. Obuszewski:** Writing – original draft; writing – review and editing; conceptualization; investigation; methodology; visualization; validation; software; formal analysis; data curation. **N. Adam Smith:** Supervision; writing – review and editing; conceptualization; investigation; methodology; project administration; resources. **Guinevere Rose Brown:** Conceptualization; writing – original draft; investigation; visualization.

## ACKNOWLEDGMENTS

We thank the Campbell Geology Museum and the North Carolina Museum of Natural Sciences for providing materials necessary for histological sampling; C. Boyd, the North Dakota Geological Survey, and the North Dakota Heritage Center for allowing study and sampling of BCGM 10272; L. Zanno for allowing use of sampling and imaging tools in the Dueling Dinosaurs Lab and providing feedback on final iterations of the manuscript; J. Anné for allowing use of sampling and imaging tools in the Dueling Dinosaurs Lab and guidance during thin section grinding and polishing stages; E. Lund for allowing use of sampling and imaging tools in the Dueling Dinosaurs Lab; A. Coulson and S. Brame for providing helpful suggestions and edits to guide the initial stages of the project; E. Bender for assisting with R-related coding and peer mentorship; E. Mulready and A. Robertson for assisting with preparation of both horncore sections; A. Tumarkin-Deratzian for helpful insight regarding squamosal histological features within BCGM 10272; W. Freimuth for thoughtful histological discussions and assistance with imaging software; and two anonymous reviewers for thoughtful and informative feedback on our manuscript. KO, NAS, and GRB completed parts of this work while in residence at Clemson University's BCGM.

## ORCID

*Kyle D. Obuszewski* https://orcid.org/0009-0007-0292-007X

## TWITTER

*Kyle D. Obuszewski* 𝕏 *kyle_obuszewski*

## REFERENCES

Ahlmann-Eltze, C., & Patil, I. (2021). ggsignif: R package for displaying significance brackets for ggplot2.

Anderson, J. S. (1999). Occipital condyle in the ceratopsian dinosaur *Triceratops*, with comments on body size variation. *Contributions from the Museum of Paleontology, University of Michigan*, *30*, 215–231.

Atterholt, J., & Woodward, H. N. (2021). A histological survey of avian post-natal skeletal ontogeny. *PeerJ*, *9*, e12160.

Baag, S. J., & Lee, Y.-N. (2022). Bone histology on *Koreaceratops hwaseongensis* (Dinosauria: Ceratopsia) from the Lower Cretaceous of South Korea. *Cretaceous Research*, *134*, 105150.

Brown, A. J., & Smith, N. (2017). Osteohistological evaluation of the squamosal in *Triceratops horridus*. *Journal of Vertebrate Paleontology, Program and Abstracts*, *2017*, 88.

Chinnery, B. J., & Horner, J. R. (2007). A new neoceratopsian dinosaur linking North American and Asian taxa. *Journal of Vertebrate Paleontology*, *27*, 625–641.

Chinsamy-Turan, A. (2005). *The microstructure of dinosaur bone: Deciphering biology with fine scale techniques* (p. 195). Johns Hopkins University Press.

D'Anastasio, R., Cilli, J., Bacchia, F., Fanti, F., Gobbo, G., & Capasso, L. (2022). Histological and chemical diagnosis of a combat lesion in *Triceratops*. *Scientific Reports*, *12*, 3941.

de Rooij, J., Lucassen, S. A. N., Furer, C., Schulp, A. S., & Sander, P. M. (2024). Exploring the ceratopsid growth record: A comprehensive osteohistological analysis of *Triceratops* (Ornithischia: Ceratopsidae) and its implications for growth and ontogeny. *Cretaceous Research*, *154*, 105738.

Farke, A. A. (2011). Anatomy and taxonomic status of the chasmosaurine ceratopsid *Nedoceratops hatcheri* from the Upper Cretaceous Lance Formation of Wyoming, U.S.A. *PLoS One*, *6*, e16196.

Farke, A. A., Wolff, E. D. S., & Tanke, D. H. (2009). Evidence of combat in *Triceratops*. *PLoS One*, *4*, e4252.

Forster, C. A. (1996a). New information on the skull of *Triceratops*. *Journal of Vertebrate Paleontology*, *16*, 246–258.

Forster, C. A. (1996b). Species resolution in *Triceratops*: Cladistic and morphometric approaches. *Journal of Vertebrate Paleontology*, *16*, 259–270.

Frederickson, J. A., & Tumarkin-Deratzian, A. R. (2014). Craniofacial ontogeny in *Centrosaurus apertus*. *PeerJ*, *2*, e252.

Fujiwara, S., & Takakuwa, Y. (2011). A sub-adult growth stage indicated in the degree of suture co-ossification in *Triceratops*. *Bulletin of the Gunma Museum of Natural History*, *15*, 1–17.

Goodwin, M. B., Clemens, W. A., Horner, J. R., & Padian, K. (2006). The smallest known *Triceratops* skull: New observations on ceratopsid cranial anatomy and ontogeny. *Journal of Vertebrate Paleontology*, *26*, 103–112.

Han, F., Zhao, Q., Hu, J., & Xu, X. (2024). Bone histology and growth curve of the earliest ceratopsian *Yinlong downsi* from the Upper Jurassic of Junggar Basin, Northwest China. *PeerJ*, *12*, e18761.

Hatcher, J. B., Marsh, O. C., & Lull, R. S. (1907). The Ceratopsia. *US Geological Survey Monograph*, *49*, 300.

Hedrick, B. P., Goldsmith, E., Rivera-Sylva, H., Fiorillo, A. R., Tumarkin-Deratzian, A. R., & Dodson, P. (2020). Filling in gaps in the ceratopsid histologic database: Histology of two basal centrosaurines and an assessment of the utility of rib histology in the Ceratopsidae. *Anatomical Record*, *303*, 935–948.

Horner, J. R., & Goodwin, M. B. (2006). Major cranial changes during *Triceratops* ontogeny. *Proceedings: Biological Sciences*, *273*, 2757–2761.

Horner, J. R., & Goodwin, M. B. (2008). Ontogeny of cranial epiossifications in *Triceratops*. *Journal of Vertebrate Paleontology*, *28*, 134–144.

Horner, J. R., & Lamm, E.-T. (2011). Ontogeny of the parietal frill of *Triceratops*: A preliminary histological analysis. *Comptes Rendus Palevol*, *10*, 439–452.

Ishikawa, H., Tsuihiji, T., & Manabe, M. (2023). *Furcatoceratops elucidans*, a new centrosaurine (Ornithischia: Ceratopsidae) from the upper Campanian Judith River Formation, Montana, USA. *Cretaceous Research*, *151*, 105660.

Klein, N., & Sander, M. (2008). Ontogenetic stages in the long bone histology of sauropod dinosaurs. *Paleobiology*, *34*, 247–263.

Lehman, T. M., Wick, S. L., & Barnes, K. R. (2017). New specimens of horned dinosaurs from the Aguja Formation of West Texas, and a revision of *Agujaceratops*. *Journal of Systematic Palaeontology*, *15*, 641–674.

Longrich, N. R., & Field, D. J. (2012). *Torosaurus* is not *Triceratops*: Ontogeny in chasmosaurine ceratopsids as a case study in dinosaur taxonomy. *PLoS One*, *7*, e32623.

Maiorino, L., Farke, A. A., Kotsakis, T., & Piras, P. (2013). Is *Torosaurus Triceratops*? Geometric morphometric evidence of Late Maastrichtian ceratopsid dinosaurs. *PLoS One*, *8*, e81608.

Mallon, J. C., Holmes, R. B., Bamforth, E. L., & Schumann, D. (2022). The record of *Torosaurus* (Ornithischia: Ceratopsidae) in Canada and its taxonomic implications. *Zoological Journal of the Linnean Society*, *195*, 157–171.

Marsh, O. C. (1889). Notice of gigantic horned Dinosauria from the Cretaceous. *American Journal of Science*, *38*, 173–176.

Napoli, J. G., Hunt, T., Erickson, G. M., & Norell, M. A. (2019). *Psittacosaurus amitabha*, a new species of ceratopsian dinosaur from the Ondai Sayr Locality, Central Mongolia. *American Museum Novitates*, *2019*, 1–36.

Padian, K., Lamm, E.-T., & Werning, S. (2013). *Bone histology of fossil tetrapods: Advancing methods, analysis, and interpretation* (p. 285). University of California Press.

Sander, P. M., & Klein, N. (2005). Developmental plasticity in the life history of a prosauropod dinosaur. *Science*, *310*, 1800–1802.

Scannella, J. B., Fowler, D. W., Goodwin, M. B., & Horner, J. R. (2014). Evolutionary trends in *Triceratops* from the Hell Creek Formation, Montana. *Proceedings of the National Academy of Sciences*, *111*, 10245–10250.

Scannella, J. B., & Horner, J. R. (2010). *Torosaurus* Marsh, 1891, is *Triceratops* Marsh, 1889 (Ceratopsidae: Chasmosaurinae): Synonymy through ontogeny. *Journal of Vertebrate Paleontology*, *30*, 1157–1168.

Scannella, J. B., & Horner, J. R. (2011). "Nedoceratops": An example of a transitional morphology. *PLoS One*, *6*, e28705.

Skutschas, P. P., Morozov, S. S., Averianov, A. O., Leshchinskiy, S. V., Ivantsov, S. V., Fayngerts, A. V., Feofanova, O. A., Vladimirova, O. N., & Slobodin, D. A. (2021). Femoral histology and growth patterns of the ceratopsian dinosaur *Psittacosaurus sibiricus* from the Early Cretaceous of Western Siberia. *Acta Palaeontologica Polonica*, *66*, 437–447.

Starck, J. M., & Chinsamy, A. (2002). Bone microstructure and developmental plasticity in birds and other dinosaurs. *Journal of Morphology*, *254*, 232–246.

Tumarkin-Deratzian, A. R. (2010). Histological evaluation of ontogenetic bone surface texture changes in the frill of *Centrosaurus apertus*. In M. J. Ryan, B. J. Chinnery-Allgeier, & D. A. Eberth (Eds.), *New perspectives on horned dinosaurs: The Royal Tyrrell Museum Ceratopsian Symposium* (pp. 251–263). Indiana University Press.

Zhao, Q., Benton, M. J., Hayashi, S., & Xu, X. (2019). Ontogenetic stages of ceratopsian dinosaur *Psittacosaurus* in bone histology. *Acta Palaeontologica Polonica*, *64*, 323–334.

## SUPPORTING INFORMATION

Additional supporting information can be found online in the Supporting Information section at the end of this article.

**How to cite this article:** Obuszewski, K. D., Smith, N. A., & Brown, G. R. (2025). An osteohistological analysis of *Triceratops* (Ornithischia: Ceratopsidae) cranial ornamentation. *The Anatomical Record*, 1–12. https://doi.org/10.1002/ar.70117